

# Integrated multilayer sputter-induced 45° YBa<sub>2</sub>Cu<sub>3</sub>O<sub>7-x</sub> grain boundary junctions

B. V. Vuchic and K. L. Merkle

*Materials Science Division and Science and Technology Center for Superconductivity, Argonne National Laboratory, Argonne, Illinois 60439*

K. A. Dean, D. B. Buchholz, R. P. H. Chang, and L. D. Marks

*Department of Materials Science and Engineering and Science and Technology Center for Superconductivity, Northwestern University, Evanston, Illinois 60208*

(Received 6 March 1995; accepted for publication 17 May 1995)

A versatile multilayer technique has been developed to form 45° YBa<sub>2</sub>Cu<sub>3</sub>O<sub>7-x</sub> [001] tilt grain boundary junctions on LaAlO<sub>3</sub> substrates. An epitaxial MgO layer is initially deposited on a (100) LaAlO<sub>3</sub> substrate using pulsed organometallic beam epitaxy (POMBE). After a pregrowth sputter treatment, an YBa<sub>2</sub>Cu<sub>3</sub>O<sub>7-x</sub> thin film is then grown using POMBE. The resultant film is *c*-axis oriented with a cube-on-cube orientation over the unsputtered portion of the MgO, and rotated by 45° about the [001] axis on the sputtered region of the substrate. The resulting grain boundary junction shows weak-link behavior. The advantage of this technique is the ability to place the grain boundary anywhere on the substrate in any configuration, and the potential to use any substrate upon which MgO can be epitaxially grown. © 1995 American Institute of Physics.

High-angle grain boundaries in the high- $T_c$  superconductors have played an important role in the development of commercial high- $T_c$  products. Most high-angle grain boundaries exhibit weak-link-type behavior which is manifested in a depressed critical current density across the boundary.<sup>1,2</sup> This is detrimental for high-current applications. These high-angle grain boundaries, however, can also be Josephson junctions which are useful in various magnetic-field and radiation sensing devices (e.g., SQUIDS). Grain boundary junctions have been formed in high- $T_c$  thin films using a variety of substrate techniques including bicrystal,<sup>2,3</sup> bi-epitaxial,<sup>4,5</sup> step-edge,<sup>6,7</sup> and sputter-induced epitaxy grain boundaries.<sup>8-10</sup> All these junctions have various types of high-angle grain boundaries formed in oriented epitaxial thin films.

One of the fundamental limitations of these junctions is the constraint on the substrate materials used. Previously reported results showed that sputter induced grain boundary junctions could be formed on MgO substrates.<sup>9,10</sup> This technique entails partially sputtering a (100) MgO substrate with low voltage argon ions (100–500 eV) prior to thin-film growth. The resulting thin film grew with a 45° rotated epitaxy on the presputtered regions of the substrate relative to the film grown on the unsputtered region. This method allows placement of multiple grain boundary junctions in virtually any configuration on the substrate and is simple to implement, but is limited to a bulk MgO substrate.

We have now developed a technique to place a grain boundary junction on a MgO layer deposited on LaAlO<sub>3</sub>. First, a layer of epitaxial MgO is deposited on LaAlO<sub>3</sub>. By sputtering a selected region of the MgO layer, the epitaxial relation between the YBa<sub>2</sub>Cu<sub>3</sub>O<sub>7-x</sub> thin film and the MgO layer can be altered to form a 45° grain boundary junction. Along with the advantages previously mentioned, the significant innovation of this method is the ability to integrate grain

boundary junctions onto a bulk substrate other than MgO. The major implication is that these junctions can be placed onto virtually any substrate upon which an (100) epitaxial MgO layer can be grown (e.g., semiconductors).

Commercially polished single-crystal (100) LaAlO<sub>3</sub> substrates were used. Between 1000 and 1500 Å of (100) epitaxial MgO were deposited using pulsed organometallic beam epitaxy (POMBE).<sup>11,12</sup> The epitaxy of the MgO film was confirmed with x-ray diffraction, the full width at half-maximum of the MgO [200]  $\Omega$ -scan rocking curve was <1° indicating a highly aligned film. The deposition of the MgO layer is described in more detail elsewhere.<sup>11</sup> The sample was then removed and physically masked by either a contact mask or using a hardbaked photoresist. The MgO layer was sputtered employing a low voltage 3 cm diam beam Kaufman-type ion source for a duration of 3 min or greater. Argon ions were used with an energy of 200–300 eV and a total beam current of 10–20 mA with a beam current density of  $\sim 1$  mA/cm<sup>2</sup>. The ion beam was incident normal to the substrate surface. The substrate was mounted with good thermal contact to a copper stage, and irradiated at room temperature with a background pressure during sputtering of  $2 \times 10^{-4}$  Torr. The physical mask was then removed, or the photoresist was dissolved in acetone. Typical step heights for a 2 min irradiation at 200 eV were 10–20 nm as determined by profilometry.

The YBa<sub>2</sub>Cu<sub>3</sub>O<sub>7-x</sub> thin films were grown using the POMBE *in situ* deposition technique as described in more detail elsewhere.<sup>12</sup> This technique allowed controlled slow growth at relatively low growth temperatures. The substrate was held at  $\sim 700$  °C during growth. The thin-film growth was assisted by an oxygen plasma. To establish reproducible conditions, the substrate was held in the oxygen plasma at the growth temperature for at least 30 min prior to thin-film growth to clean the substrate surface. The ambient gas in the

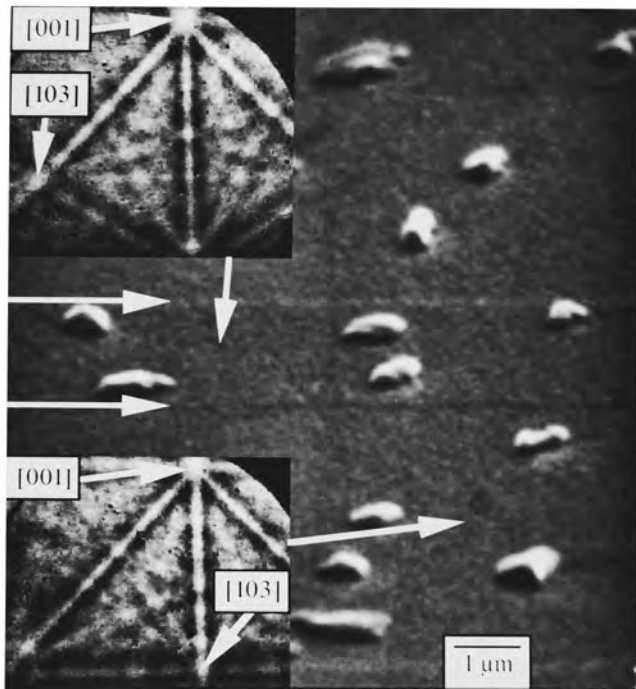


FIG. 1. A secondary electron image of two parallel grain boundary junctions (shown with arrows) with corresponding backscattered electron Kikuchi patterns indicating a  $45^\circ$  rotation about the [001] axis in adjacent grains.

growth chamber during deposition was  $\sim 70\%$  oxygen,  $28\%$  helium, and  $2\%$  water vapor. The deposition rates of the films varied from 3 to  $11 \text{ \AA}/\text{min}$ . The film thicknesses were between 2000 and  $3000 \text{ \AA}$ . The orientation of the film was determined with backscattered electron Kikuchi patterns in a JEOL 6400 scanning electron microscope (SEM) (see Fig. 1).<sup>13</sup>

Low-temperature four probe transport measurements were made to determine current–voltage and resistance–temperature characteristics. The samples were patterned for transport measurements with a molybdenum contact mask with a  $35 \text{ }\mu\text{m}$  wide microbridge. Argon ion milling was used to remove the exposed regions of the thin film. The microbridge allowed for independent transport measurement across the grain boundary and within the two grains adjacent to the grain boundary. The contact pads were cleaned with a low energy ion beam and then silver contacts were evaporated *in situ*. Gold leads were connected to the sample using silver paint. Standard four probe dc measurements were performed in a cold finger flow cryostat. A  $1 \text{ }\mu\text{V}$  criterion was used in determining the critical current from the current–voltage ( $I$ – $V$ ) measurements.

After deposition of the  $\text{YBa}_2\text{Cu}_3\text{O}_{7-x}$  thin film, backscattered electron Kikuchi patterns were used to confirm the thin-film orientation. Figure 1 shows a secondary electron image of the sample (the sample was inclined  $70^\circ$  relative to the electron beam to optimize backscattered electron detection and to increase the contrast from the grain boundary) with the corresponding backscattered electron Kikuchi patterns. The bright spots in Fig. 1 are small precipitates of copper oxide formed due to excess copper during deposition. The concentration of precipitates is highly dependent on the specific deposition conditions. The sharpness of the ground

boundaries in Fig. 1 which border a  $5 \text{ }\mu\text{m}$  wide presputtered strip indicates that the technique is probably limited by the physical mask quality. The orientation over the unsputtered region of the MgO layer was (001)  $\text{YBa}_2\text{Cu}_3\text{O}_{7-x} \parallel (001) \text{ MgO}$  and (100)  $\text{YBa}_2\text{Cu}_3\text{O}_{7-x} \parallel (100) \text{ MgO}$ . The film on the presputtered region of MgO was rotated by  $45^\circ$  about the [001] axis and had the orientation relation of (001)  $\text{YBa}_2\text{Cu}_3\text{O}_{7-x} \parallel (001) \text{ MgO}$  and (100)  $\text{YBa}_2\text{Cu}_3\text{O}_{7-x} \parallel (110) \text{ MgO}$ . Therefore, a  $45^\circ$  [001] tilt grain boundary was formed at the interface between the film grown on the presputtered region and the unsputtered region of the MgO.

It is known that  $\text{YBa}_2\text{Cu}_3\text{O}_{7-x}$  grows in several different epitaxial orientations on (100) MgO substrates depending on the growth conditions.<sup>14–16</sup> The  $45^\circ$  rotated epitaxial relation is probably energetically close to the cube-on-cube relation despite the large lattice mismatch between the MgO and the  $\text{YBa}_2\text{Cu}_3\text{O}_{7-x}$  because it is often found in  $\text{YBa}_2\text{Cu}_3\text{O}_{7-x}$  thin films grown under various conditions without a sputter pretreatment. It appears that the presputter modifies the surface in such a manner as to make the  $45^\circ$  rotated epitaxy more favorable than the cube-on-cube orientation.

The technique used for the presputter treatment and the resulting thin-film orientation is shown schematically in Fig. 2. The backscattered electron Kikuchi patterns confirmed that the rotation occurred across the entire presputtered region and was maintained up to the grain boundary without any small unrotated grains. The grain boundaries in Fig. 1 showed little grain boundary contrast indicating a very smooth film. Films with such grain boundaries have been consistently formed over a period of several months using this technique.

The resistance–temperature curves of an individual grain boundary junction and the adjacent grain are shown in Fig. 3. The critical temperature in the grain is  $\sim 89 \text{ K}$ . In the grain boundary there is an abrupt decrease in resistivity as a function of temperature, corresponding to the transition to the superconducting state in the two grains surrounding the grain boundary. However, the grain boundary remains resistive until  $\sim 83 \text{ K}$ . This footlike structure is associated with the grain boundary resistance and has been attributed to thermally activated phase slippage by other authors.<sup>17</sup> The foot structure is typical for grain boundary junctions and is dependent on the current used in the measurement of the resistance.

The current–voltage characteristics for various temperatures are shown in Fig. 4. The grain boundary critical current is significantly less than the grain critical current (which was never reached due to the possibility of destroying the junction from resistive heating). The critical current density values of the grain boundary are  $5 \times 10^3 \text{ A}/\text{cm}^2$  at  $5 \text{ K}$  and decrease to  $7 \times 10^2 \text{ A}/\text{cm}^2$  at  $60 \text{ K}$ . The  $I$ – $V$  curve shows RSJ-like behavior at low temperature, but begins rounding at  $60 \text{ K}$  indicating more of a flux-flow-type behavior. The  $I_c R_n$  product is  $52.5 \text{ }\mu\text{V}$  at  $10 \text{ K}$  and decreases to  $8 \text{ }\mu\text{V}$  at  $60 \text{ K}$ . The relatively low  $J_c$  and  $I_c R_n$  products are due primarily to the grain boundary geometry. Grain boundary junctions with a  $45^\circ$  misorientation have been shown to have low critical currents.<sup>2–5</sup> Although the critical currents observed are somewhat lower than the best values for the sputter-induced

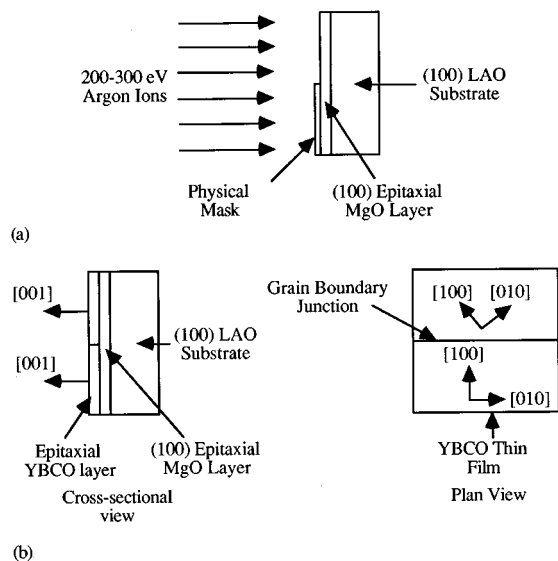


FIG. 2. Schematic diagram showing (a) the low voltage argon ion pretreatment configuration and (b) the resulting thin-film orientation after deposition.

grain boundary junctions made on bulk single-crystal MgO substrates (grain boundary  $J_c = 5 \times 10^4$  at 4.2 K and  $1.6 \times 10^3$  A/cm<sup>2</sup> at 77 K), we believe that by improving the quality of the MgO layer, the grain boundary junction can also be improved to the same values.

Sputter-induced epitaxy has only been attempted using the POMBE system. Currently both sputter deposition and pulsed laser deposition techniques are being investigated to determine whether the technique is compatible with other growth methods. Also, SrTiO<sub>3</sub> and GaAs bulk substrates are being studied as base substrates.

The ability to place a grain boundary junction on a multilayer substrate gives tremendous versatility to this technique. Hence, the grain boundary junction can be a part of a multilayer scheme which can be placed on any substrate as long as an epitaxial layer of MgO can be grown. Thus, a

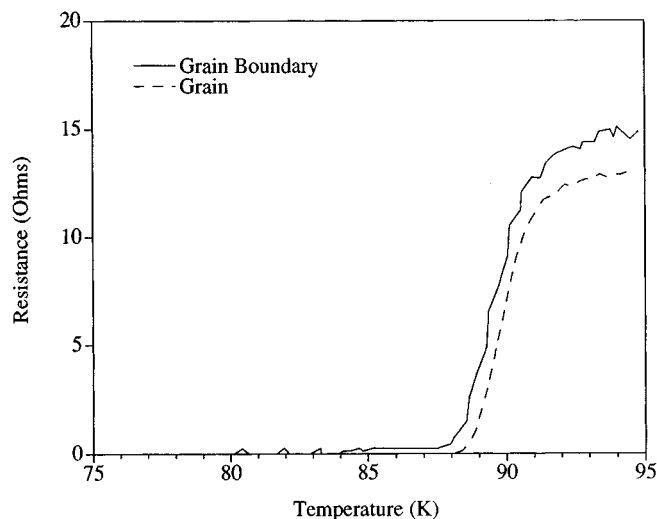


FIG. 3. Resistance vs temperature characteristics for the grain boundary junction and the grain.

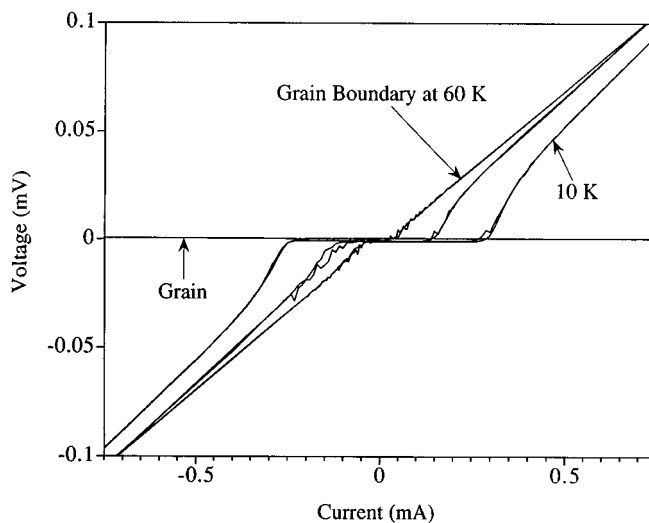


FIG. 4. Voltage vs current characteristics at 10, 40, and 60 K for the grain and grain boundary. The microbridge is 35  $\mu$ m wide.

simple way has been found to integrate high- $T_c$  junctions with various other substrate materials that can be tailored to the specific system requirements.

This work was supported by the National Science foundation Office of Science and Technology Centers, under Contract No. DMR 91-20000 (B.V.V., K.A.D., D.B.B., R.P.H.C., and L.D.M.) and the U.S. Department of Energy, Basic Energy Sciences-Materials Science, under Contract No. W-31-109-ENG-38 (K.L.M.).

- <sup>1</sup>D. Dimos, P. Chaudhari, J. Mannhart, and F. K. LeGoues, Phys. Rev. Lett. **61**, 219 (1988).
- <sup>2</sup>D. Dimos, P. Chaudhari, and J. Mannhart, Phys. Rev. B **41**, 4038 (1990).
- <sup>3</sup>Z. G. Ivanov, P. Å. Nilsson, D. Winkler, J. A. Alarco, T. Claeson, E. A. Stepantsov, and A. Y. Tzalenchuk, Appl. Phys. Lett. **59**, 3030 (1991).
- <sup>4</sup>K. Char, M. S. Colclough, S. M. Garrison, N. Newman, and G. Zaharchuk, Appl. Phys. Lett. **59**, 733 (1991).
- <sup>5</sup>K. Char, M. S. Colclough, L. P. Lee, and G. Zaharchuk, Appl. Phys. Lett. **59**, 2177 (1991).
- <sup>6</sup>C. L. Jia, B. Kabius, K. Urban, K. Herrmann, G. J. Cui, J. Schubert, W. Zander, A. I. Braginski, and C. Heiden, Physica C **175**, 543 (1991).
- <sup>7</sup>K. P. Daly, W. D. Dozier, J. F. Burch, S. B. Coons, R. Hu, C. E. Platt, and S. W. Simon, Appl. Phys. Lett. **58**, 543 (1991).
- <sup>8</sup>N. G. Chew, S. W. Goodyear, R. G. Humphreys, J. S. Satchell, J. A. Edwards, and M. N. Keene, Appl. Phys. Lett. **60**, 1516 (1992).
- <sup>9</sup>B. V. Vuchic, K. L. Merkle, K. A. Dean, D. B. Buchholz, R. P. H. Chang, and L. D. Marks, J. Appl. Phys. **77**, 2591 (1995).
- <sup>10</sup>B. V. Vuchic, K. L. Merkle, J. W. Fundhouser, D. B. Buchholz, K. A. Dean, R. P. H. Chang, and L. D. Marks, IEEE Trans. Appl. Supercond. (to be published).
- <sup>11</sup>K. A. Dean, D. B. Buchholz, L. D. Marks, R. P. H. Chang, B. V. Vuchic, K. L. Merkle, D. B. Studebaker, and T. J. Marks (unpublished).
- <sup>12</sup>D. B. Buchholz, S. J. Duray, D. L. Schulz, T. J. Marks, J. B. Ketterson, and R. P. H. Chang, Mater. Chem. Phys. **36**, 377 (1994).
- <sup>13</sup>J. A. Venables and C. J. Harland, Philos. Mag. **27**, 1193 (1973).
- <sup>14</sup>S. McKernan, M. G. Norton, and C. B. Carter, J. Mater. Res. **7**, 1052 (1992).
- <sup>15</sup>D. M. Hwang, T. S. Ravi, R. Ramesh, S.-W. Chan, C. Y. Chen, L. Nazar, X. D. Wu, A. Inam, and T. Venkatesan, Appl. Phys. Lett. **57**, 1690 (1990).
- <sup>16</sup>D. H. Shin, J. Silcox, S. E. Russek, D. K. Lathrop, B. Moeckly, and R. A. Buhrman, Appl. Phys. Lett. **57**, 508 (1990).
- <sup>17</sup>R. Gross, in *Interfaces in Superconducting Systems*, edited by S. L. Shinde and D. Rudman (Springer, New York, 1992), p. 1.